Resonant Rayleigh Scattering from Bilayer Quantum Hall Phases

Stefano Luin,[1,2] Vittorio Pellegrini,[1] Aron Pinczuk,[3,2] Brian S. Dennis,[2] Loren N. Pfeiffer,[2] and Ken W. West[2]

[1]*NEST CNR-INFM and Scuola Normale Superiore, Piazza dei Cavalieri 7, I-56126 Pisa, Italy*

[2]*Bell Labs, Lucent Technologies, Murray Hill, New Jersey 07974, USA*

[3]*Department of Physics, Department of Applied Physics and Applied Mathematics, Columbia University, New York, New York 10027, USA*

(Received 12 June 2006; published 21 November 2006)

We observe resonant Rayleigh scattering of light from quantum Hall bilayers at Landau level filling factor $\nu = 1$. The effect arises below 1 Kelvin when electrons are in the incompressible quantum Hall phase with strong interlayer correlations. Marked changes in the Rayleigh scattering signal in response to application of an in-plane magnetic field indicate that the unexpected temperature dependence is linked to formation of a nonuniform electron fluid close to the phase transition towards the compressible state. These results demonstrate a new realm of study in which resonant Rayleigh scattering methods probe quantum phases of electrons in semiconductor heterostructures.

DOI: 10.1103/PhysRevLett.97.216802 PACS numbers: 73.43.Fj, 73.43.Nq, 78.35.+c

The elastic scattering of radiation is an elementary process that was described by Lord Rayleigh [1]. Elastic (Rayleigh) scattering occurs in inhomogeneous condensed matter systems and in crystals with defects. Resonant Rayleigh light scattering (RRS) was also reported in semiconductor quantum wells at temperatures of several degrees Kelvin [2] and explained by inhomogeneous fluctuations in quantum well width that cause the localization of optical excitons [2–4]. Rayleigh scattering of light has found remarkable application in the study of classical phase transitions and critical phenomena in gases and liquids [5,6].

Here we report the observation of RRS at mK temperatures in electron bilayers confined in double quantum wells (DQW) at filling factor $\nu = 1$ ($\nu = 2\pi n l_B^2$, $l_B^2 = \hbar c/eB$, n is the electron density and B the perpendicular magnetic field [7]). The phases of the bilayers at $\nu = 1$ are determined by d/l_B (d is the interlayer distance) and $\Delta_{\mathrm{SAS}}/E_C$ where Δ_{SAS} is the tunneling gap and $E_C = e^2/\varepsilon l_B$. A phase transition shown in Fig. 2(c) separates a quantum Hall (QH) phase stabilized by strong interlayer correlations (at small d/l_B or large $\Delta_{\mathrm{SAS}}/E_C$) from a compressible state determined by intralayer correlations [8]. The RRS is seen close to this phase transition when the bilayers are in the incompressible quantum Hall (QH) phases that occur at finite values of the tunneling gap Δ_{SAS}. These are remarkable correlated states of electrons that display occupation of Landau levels that departs from the conventional filling in which only the lowest Landau level is populated [9]. The photon energy of the maximum RRS enhancement overlaps that of magneto-optical transitions in the quantum well structures. These measurements show that the large, resonantly enhanced, Rayleigh scattering intensities seen at 60 mK disappear as the temperature approaches 1 K.

We demonstrate that the RRS intensity and its temperature dependence display remarkable changes when Δ_{SAS} is decreased by the application of in-plane components of magnetic field ($B_\parallel$). The evolution of RRS marks the occurrence of the phase transition at a critical value of $B_\parallel$ when the electron bilayers at $\nu = 1$ enter the compressible regime due to the reduction of the tunneling gap [8,9]. This behavior links the origin of the observed RRS to a nonuniform spatial structure of the incompressible QH electron fluid close to the phase transition. These results agree well with recent predictions of separation into incompressible and compressible domains close to the $\nu = 1$ phase transition of electrons bilayers [10–13]. The resonant Rayleigh scattering results thus uncover a new domain of applications in which RRS effects probe quantum phases of electrons that emerge at low temperatures in semiconductor structures.

Samples kept in a dilution refrigerator with windows for optical access and base temperature below 50 mK were tilted with respect to the magnetic field direction (with perpendicular and in-plane components given by $B = B_T \cos\theta$ and $B_\parallel = B_T \sin\theta$). B was always chosen to correspond to $\nu = 1$ for all values of tilt angle θ. The photon energies of the emission of dye, diode, or titanium-sapphire lasers were tuned close to the fundamental interband optical gap of the double quantum well ($\lambda \approx 810$ nm). The in-plane wave-vector transfer in the light scattering in the backscattering geometry employed here is given by $q = |k_S^\parallel - k_L^\parallel| = 4\pi \sin(\theta)/\lambda$, where $k_{S(L)}^\parallel$ is the in-plane projection of the wave vector of the scattered (laser) light. The nonspecular scattered light was collected into a double or triple spectrometer equipped with a CCD detector with spectral resolution of 15 μeV. A crossed polarization scheme was adopted in order to reduce the impact of the stray laser light collected by the spectrometer.

Two nominally symmetric modulation-doped $Al_{0.1}Ga_{0.9}As/GaAs$ DQWs were studied with total electron densities of $n = 1.2 \times 10^{11}$ cm^{-2} (sample 1) and $n = 1.1 \times 10^{11}$ cm^{-2} (sample 2) and d/l_B (at $\nu = 1$) of 2 and

2.2, respectively. The values of Δ_{SAS} are 0.58 meV (sample 1) and 0.36 meV (sample 2). The lowest-lying spin excitations at $\nu = 1$, that are detected together with RRS, are the spin-flip (SF) mode across Δ_{SAS} with simultaneous change of spin and, at lower energy, the spin-wave (SW) mode across the Zeeman gap [9]. The transitions that build SW and SF modes are shown in Fig. 1(a).

Figure 1(c) displays a resonant enhancement profile of Rayleigh scattering intensity in sample 1 at an incident laser intensity of $\sim 10^{-4}$ W/cm^2 and $\theta = 30°$. The peaks that have line-width limited by the resolution of the spectrometer are plotted for different incident laser wavelengths and compared to the broad luminescence profile of the $\nu = 1$ QH fluid. The sharp resonant profile of the Rayleigh intensity (FWHM of approximately 1–2 Å $\sim$ 0.2–0.4 meV) and the photon energy of maximum enhancement located on the high-energy side of the luminescence indicate that the Rayleigh scattering relies on an interband excitonic resonance of the semiconductor heterostructures. In this exciton the electron states are in the first excited Landau level as shown in Fig. 1(b).

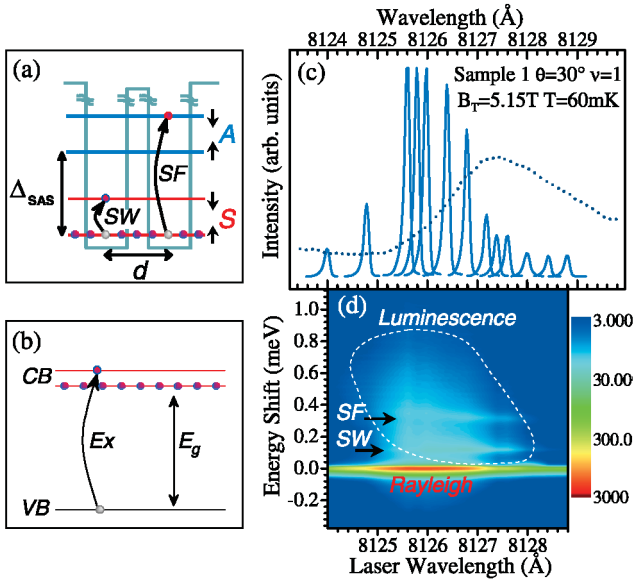

FIG. 1 (color). (a) Schematic view of the double quantum well at $\nu = 1$. Transitions in the SW and SF modes are indicated. Short vertical arrows indicate the orientation of spins, symmetric (S) and antisymmetric (A) states are separated by the tunneling gap Δ_{SAS}. (b) Transitions that contribute to the interband magnetoexciton (Ex) responsible for the resonance in the Rayleigh scattering intensity. The red lines represent Landau levels. Valence (VB) and conduction bands (CB) are separated by the interband gap E_g. (c) Representative example of the resonant profile of the Rayleigh scattering intensity at $\nu = 1$ and $T = 60$ mK: each sharp peak is the elastically scattered light with wavelengths and line shapes that match the ones of the incoming laser light. The dotted line is the magnetoluminescence with off-resonant excitation. (d) Logarithmic scale color plot of the light scattering intensities for the case reported in (c). The horizontal scale is the incident laser wavelength and the vertical scale is the energy shift between the scattered and incident light. The resonant Rayleigh scattering occurs at zero energy shift. Also indicated are the SW and SF inelastic light scattering peaks and the incoherent emission due to luminescence.

The color plot in Fig. 1(d) reports the light scattering intensity in sample 1 as a function of the incident laser wavelength (horizontal axis) and of the shift between the scattered and incident photon energies (vertical axis). RRS occurs at zero energy shifts. At positive energy shifts we also observe an optical recombination emission due to magneto luminescence and the inelastic light scattering signals due to SF and SW excitations. The energy splitting between these two excitations is much smaller than the value of $\Delta_{SAS} = 0.58$ meV expected from the picture shown in Fig. 1(a) and from mean-field theories [14]. The reduction of the energy splitting implies that a fraction of electrons occupies the higher-energy spin-up antisymmetric Landau level in this correlated QH phase [9,15]. The occurrence of the QH effect at $\nu = 1$ thus suggests those electrons to be bound to the holes left behind in the lowest-energy symmetric Landau level to create neutral excitoniclike particles not contributing to charge transport [9].

Figure 2 shows the marked temperature dependence of the RRS intensity. Results refer to sample 2. At the lowest tilt angle of $\theta = 5°$ the RRS disappears above $T = 0.8$ K [Fig. 2(a) and top curve in Fig. 2(d)]. When Δ_{SAS} is reduced by increasing $B_{\|}$ [16], the evolution becomes

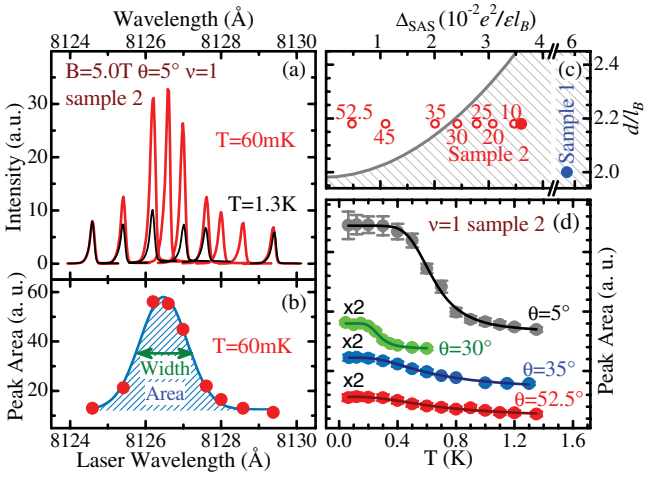

FIG. 2 (color online). (a) Evolution of the Rayleigh scattering peaks as a function of incident laser wavelength at two different temperatures for sample 2 and (b) resonant profile for the Rayleigh scattering at $T = 60$ mK. (c) Phase diagram for the incompressible (shaded area) and compressible (white area) states of the bilayer at $\nu = 1$ [8]. The blue and red dots refer to samples 1 and 2, respectively. The sequence of open circles marks the evolution of the position of sample 2 at different angles θ (values in degrees). (d) Temperature behavior of the resonant Rayleigh scattering at different angles for sample 2. The best fits to Eq. (1) reported in the text are shown as solid lines. Data at each angle are shifted vertically for clarity.

more pronounced with the RRS disappearing just above 0.4 K at $\theta = 30°$. As θ becomes equal or larger than the critical value of $\theta_c \approx 35°$ ($\Delta_{SAS}/E_C = 0.018$) [9] both the RRS intensity, its resonant profile and temperature behavior change abruptly signaling the occurrence of a phase instability. At this critical value of Δ_{SAS}/E_C the position of sample 2 crosses the incompressible-compressible phase boundary [Fig. 2(c)] [8,17].

The dependence of the RRS intensity on temperature and $B_{\|}$ shown in Fig. 2 are nearly identical to those of spin excitations that are characteristic signatures of highly correlated bilayer QH phases [9]. The results in Fig. 2 thus establish an unambiguous link between RRS and the phase transformations of the correlated bilayer QH fluids into compressible states. The results shown in Figs. 3(a) and 3(b), that compare the RRS at representative angles below and above θ_c, provides key evidence on the nature of the quantum phase that emerges above θ_c: the vanishing of the resonant component of the Rayleigh scattering intensity for angles $\theta \geq \theta_c$ indicates that the emergent phase is significantly more homogeneous than the bilayer QH phase that occurs for $\theta < \theta_c$.

The occurrence of the phase transition to the compressible state implies that the nonuniform phase yielding RRS consists of compressible and incompressible domains with two characteristic lengths ξ_1 and ξ_2, and average distance $\xi_1 + \xi_2$ [3,18]. A spatial variation in the dielectric constant $\Delta\epsilon$ arises because the interband magneto-excitons responsible for the resonant enhancement exist in the incompressible regions only while excitonic interaction is screened in the compressible domains. The θ -dependence of the RRS intensity requires changes in ξ_1 and ξ_2 that occur when $B_{\|}$ is changed. The maximum RRS intensity in the far field is obtained when ξ_1 and ξ_2 are comparable and close to $\lambda/2\pi \sin(\theta)$ ($\approx$700 nm at 10°) [18]. While a precise determination of the scale of disorder from RRS requires more work [19], the submicron sizes of the inhomogeneities estimated above are consistent with those deduced independently from the line shape fitting of SF and SW excitations. The fitting is based on time-dependent Hartree-Fock analysis. It incorporates higher-energy spin excitations at finite wave vectors due to disorder-induced breakdown of wave vector conservation in the inelastic light scattering process [20].

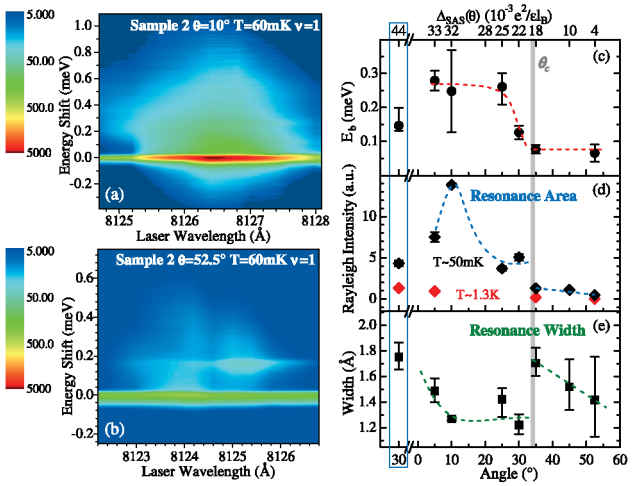

FIG. 3 (color). (a) and (b) show color plots of RRS at $T = 60$ mK at $\theta < \theta_c$ and $\theta > \theta_c$, respectively. The sharp resonant enhancement of RRS observed in (a) disappears above $\theta_c = 35°$. (c) Evolution of the binding energy E_b [defined in Eq. (1)] as a function of angle (bottom horizontal axis) and Δ_{SAS}/E_C (top horizontal axis). Data are in sample 2 except for the points in the blue rectangle that refer to sample 1 at $\theta = 30°$. (d),(e) same as in (c) but for the Rayleigh intensity (d) and resonance width (e) as obtained as in Fig. 2(b).

To interpret the temperature dependence we recall that in the range of the Δ_{SAS} and d/l_B values of our samples and below θ_c the bilayer electron fluid at $\nu = 1$ is in the QH phase [8,9]. This indicates that the dominant domains stable at low-temperature are in the correlated QH state described in Ref. [9] and create a percolation path throughout the sample allowing charge transport consistent with the QH effect.

The RRS intensity decreases monotonically for both samples at all angles, and its temperature behavior is similar to that of other characteristic signatures of the QH effect. This suggests that the temperature dependence is more influenced by changes in the optical response of the incompressible domains rather than by changes in the dimensions of the domains. It is conceivable that thermally activated free charged excitations in the QH domains could screen the interband excitons reducing the mismatch $\Delta\epsilon$ among the two domains thus suppressing the RRS.

In order to be more quantitative, we fitted the RRS intensity with the 2D version of the Langmuir adsorption isotherm. This function was applied to describe thermally induced exciton delocalization in quantum wells [21]. In this framework the T dependence of the resonant Rayleigh intensity I_{RRS} is given by

$$I_{RRS}(T) = \frac{I^0_{RRS}}{1 + CT\exp(-E_b/kT)}. \quad (1)$$

In Eq. (1) E_b is a binding energy to localization sites and $C = 2\pi M k_B/N_p h^2$, where N_p can be viewed as the density of binding sites and M the mass of the bound particle. Within the mechanism suggested above E_b is also linked to the energy required to inject free charge in the incompressible domains. The solid black line on the top of Fig. 2(d) represents the best fit of the experimental RRS intensities to Eq. (1) at $\theta = 5°$. The best-fit analysis yields $E_b = 0.27$ meV (3.3 K), $C = 0.2$ K^{-1} and $N_p = 6 \times 10^9$ cm^{-2} assuming $M = m_e = 0.067 m_0$ (where m_0 is the free electron mass). The values for E_b in the incompressible states are indeed similar to those found in thermoactivated transport experiments in QH bilayers at $\nu = 1$ [22]. It is also intriguing to link this transition to a cooperative phenome-

non of ionization of the excitons reported in Ref. [9]. To this end we note that typical excitonic binding energies calculated for sample 2 within a time-dependent Hartree-Fock approach are consistent with the value of $E_b = 0.27$ meV [14,23].

The temperature dependences can be fitted by Eq. (1) at all tilt angles. However, while below θ_c the values of C range between $C = 0.1$ K^{-1} and $C = 4$ K^{-1} ($N_p \approx 3 \times 10^8$–$1.2 \times 10^{10}$ cm^{-2}, corresponding to a scale for the disorder of 90–600 nm), at angles of $\theta_c \approx 35°$ or above the fit yields $C = 0.006$ K^{-1} or less [scale for the disorder less than 10(20) nm using the effective exciton(electron) mass for M [21]] signaling the emergence of a different physical configuration. Solid lines in Fig. 2(d) represent the best-fit to Eq. (1) at different angles. Figures 3(c)–3(e) report the values of the binding energy E_b, I^0_{RRS}, and RRS linewidth versus angle or versus $\Delta_{\mathrm{SAS}}(\theta)/E_c$. The phase transition at θ_c is signaled by a smooth decrease of the binding energy and abrupt changes of I^0_{RRS} and RRS linewidth. In addition, the photon energy of the maximum enhancement of the residual weak Rayleigh scattering above θ_c overlaps that of the luminescence peak maximum indicating a resonant mechanism different from that shown in Fig. 1(b). Figure 3(d) also reports the RRS intensity values at 1.3 K. At this temperature the RRS displays a marginal resonant effect and angle dependence. Figure 3(d) highlights the absence of a significant temperature dependence of RRS in the phase above θ_c.

A candidate state for the competing minority domains at low-temperature for $\theta < \theta_c$ is the compressible state composed by two weakly interacting composite-fermion systems (each of them at $\nu = 1/2$) [12]. It is possible that spontaneous phase separation occurs in the vicinity of the phase instability and that at $\theta > \theta_c$ the critical proliferation of such domains leads to a more homogeneous compressible fluid with marginal RRS. It is also possible that weak residual disorder in the QH phase [24,25] could lead to coexistence of QH domains at $\nu = 1$ with non-QH domains at $\nu \neq 1$. Above $\theta \geq \theta_c$, however, even the $\nu = 1$ domains should not be in the QH phase and this would create a more homogeneous fluid suppressing the RRS.

In conclusion, we discovered a large resonant Rayleigh signal with unusual temperature dependence linked to the $\nu = 1$ phase transition in QH bilayers. The resonant Rayleigh scattering reported here opens new venues for the study of macroscopic coherence in QH bilayers and of other quantum phases of electrons in low-dimensional semiconductor heterostructures.

We are grateful to Steven H. Simon for critical reading of the manuscript. V. P. acknowledges the support of the Italian Ministry of Foreign Affairs, the Italian Ministry of Research and by the European Community Human Potential Programme (Project No. HPRN-CT-2002-00291). A. P. acknowledges the National Science Foundation under Grant No. DMR-03-52738, the Department of Energy under Grant No. DE-AIO2-04ER46133, the Nanoscale Science and Engineering Initiative of the National Science Foundation under Grant No. CHE-0117752, and a research grant of the W. M. Keck Foundation.

[1] Lord Rayleigh, Philos. Mag. **47**, 375 (1899).
[2] J. Hegarty *et al.*, Phys. Rev. Lett. **49**, 930 (1982).
[3] H. Stolz *et al.*, Phys. Rev. B **47**, 9669 (1993).
[4] D. Birkedal and J. Shah, Phys. Rev. Lett. **81**, 2372 (1998).
[5] I. J. Fritz and H. Z. Cummins, Phys. Rev. Lett. **28**, 96 (1972); S. Takagi and H. Tanaka, Phys. Rev. Lett. **93**, 257802 (2004); B. J. Berne and R. Pecora, *Dynamic Light Scattering* (Wiley, New York, 1976).
[6] T. Andrews, Phil. Trans. R. Soc. London **159**, 575 (1869).
[7] R. E. Prange and S. M. Girvin, *The Quantum Hall Effect* (Springer, New York, 1990), 2nd ed.
[8] S. Q. Murphy *et al.*, Phys. Rev. Lett. **72**, 728 (1994).
[9] S. Luin *et al.*, Phys. Rev. Lett. **94**, 146804 (2005).
[10] A. Stern and B. I. Halperin, Phys. Rev. Lett. **88**, 106801 (2002).
[11] M. Kellogg *et al.*, Phys. Rev. Lett. **90**, 246801 (2003).
[12] S. H. Simon *et al.*, Phys. Rev. Lett. **91**, 046803 (2003).
[13] H. A. Fertig and G. Murthy, Phys. Rev. Lett. **95**, 156802 (2005).
[14] L. Brey, Phys. Rev. Lett. **65**, 903 (1990).
[15] M. Polini *et al.*, Solid State Commun. **135**, 654 (2005).
[16] J. Hu and A. H. MacDonald, Phys. Rev. B **46**, 12 554 (1992).
[17] S. Luin *et al.*, Physica E (Amsterdam) **34**, 244 (2006).
[18] If we consider an incident cw laser excitation and a backscattered wave, the Rayleigh scattering intensity I^o_{RRS} in far field, within the Born approximation and with a Gaussian distribution for the dimensions of the two domains, is proportional to $\Delta\epsilon^2 \frac{\xi_1^2\xi_2^2}{(\xi_1^2+\xi_2^2)} \times [\xi_1^4 \exp(-q^2\xi_1^2/4) + \xi_2^4 \exp(-q^2\xi_2^2/4)]$, where $\Delta\epsilon$ is the difference of the frequency-dependent dielectric constants in the two domains.
[19] See for instance, W. Langbein *et al.*, Phys. Rev. Lett. **82**, 1040 (1999).
[20] I. K. Marmorkos and S. Das Sarma, Phys. Rev. B **45**, 13 396 (1992).
[21] J. E. Zucker *et al.*, Phys. Rev. B **35**, 2892 (1987).
[22] T. S. Lay *et al.*, Phys. Rev. B **50**, 17 725 (1994).
[23] S. Luin *et al.*, Phys. Rev. Lett. **90**, 236802 (2003).
[24] S. Ilani *et al.*, Nature (London) **427**, 328 (2004); J. Martin *et al.*, Science **305**, 980 (2004).
[25] G. A. Steele *et al.*, Phys. Rev. Lett. **95**, 136804 (2005).